Transactions of the Materials Research Society of Japan 35[4]801-804(2010)

Numerical simulation of welding fume formation mechanism in gas tungsten arc welding

Tasuku Zeniya*, Shinichi Tashiro, Kentaro Yamamoto, Manabu Tanaka, Kazuhiro Nakata, Eri Yamamoto [a], Kei Yamazaki [a], Keiichi Suzuki [a],
Joining and Welding Research Institute, Osaka University 11-1 Mihogaoka, Ibaraki, Osaka 576-0047, Japan
Fax: +81-6-6879-8666, e-mail: zeniya@jwri.osaka-u.ac.jp
[a] KOBE STEEL, LTD. 100-1, Miyamae, Fujisawa, Kanagawa, 251-8551, Japan

In a GTA (Gas Tungsten Arc) welding, large amount of high temperature metal vapor is generated from the melting tip of a welding wire, a droplet and a weld pool. In this process, high temperature metal vapor is cooled rapidly and oxidized during diffusion to the surrounding air. Then a primary particle (nanoparticle), whose size is approximately 1nm~100nm, is formed through a nucleation. Furthermore, a part of these particles condenses and produces a secondary particle whose maximum size is over 1μm. It becomes the form of smoke and rises with the ascending current from the high temperature weld pool. They are called welding fume. For reducing the quantity and controlling the size of the fume, we integrated a fume formation model and visualized the fume formation process. Simulation was calculated changing physical property. Fig. 1 represents a secondary particle. The secondary particles with beaded (chain-like) shape composed of small particles whose sizes are approximately below 100nm were observed. As a result, it was confirmed that the shapes and the sizes of the secondary particles obtained in the simulation approximately agrees with that in the experiment.
Key words: Fume, Metal vapor, Arc, Numerical analysis

1. INTRODUCTION

In the arc welding process, welding workers can't avoid inhaling welding fume. As measures to this problem, a welding fume collector or a fume mask etc is generally used. However the environment, where the welding fume collector is used in, is limited because the collector is expensive and large size and, furthermore, disturbs the plasma flow. On the other hand, the mask is cheap and used generally but complete collecting is extremely difficult. Therefore, an improvement in welding environmental becomes an important theme. In order to accomplish this theme, it is necessary not only to reduce the quantity of the welding fume but also to decrease a content of nanoparticles with small size because there is particularly high degree of risk to the human body due to inhalation. Furthermore, the technology for controlling the particle size to improve the collecting rate with the mask is indispensable.

Recently, some studies were conducted about nanoparticle formation mechanism in the similar situation such as the welding. Watanabe carried out an experiment and a simulation on the nanoparticle generation of alloy and intermetallics in thermal plasma [1]. Furthermore, Shigeta simulated co-condensation growth of multi-component nanoparticles in thermal plasma processing by a two-directional nodal model for easy-to-use [2]. In addition, Girshick researched dependence of nanoparticle formation mechanism on the distance from an induction coil, the discrimination time of the particle, the cooling rate and the partial pressure of the iron vapor [3].

Jenkins reported that welding fume is not good for health of workers because it contains various kinds of detrimental element and it is important to know the composition and the size of the welding fume. Thus, he analyzed welding fume in GMAW (Gas Metal Arc Welding) and SMAW (Shielded Metal Arc Welding) with a spectrum analyzer called EDS (Energy Disper-sive Spectrometry) [4]. However, the research about a nanoparticle formation in the welding was conducted mainly by the experiment.

In this paper, reducing the quantity and controlling the size of the welding fume are aimed by simulation. We integrated a secondary particle model with a primary particle model and visualized the second particle coagulation process for observing the shapes of the secondary particle. In order to understand the welding fume formation mechanism, we tried elucidation of the fume formation mechanism by this model.

2. SIMULATION MODEL

We used a formation model that the fume is generated from metal vapor by the arc. As the process of nanoparticle formation, the assumptions (1)~(5) are employed.

(1) The formation of supersaturation of the metal vapor by cooling.
(2) The formation of the primary particle by the homogeneous nucleation.
(3) The growth of the primary particle by the heterogeneous condensation.
(4) The formation of the secondary particle by the coagulation.

(5) The growth of the secondary particle by the heterogeneous condensation and the coagulation.

2.1 Homogeneous Nucleation Model of Primary Particle

In theory, the homogeneous nucleation can arise if the degree of supersaturation exceeds 1. It is assumed that the nucleus with a critical diameter d_p is created due to the nucleation. It is the smallest nucleus's diameter which there can be a nucleus stably, and is represented by equation (1)

$$d_p = \frac{4\sigma v_m}{kT \ln S} \tag{1}$$

where σ(N/m) is surface tension, v_m (/m^3) is volume of the liquid molecule, k is the Boltzmann constant, S is degree of supersaturation. In addition, in this paper, we referred to a Friendlander's liquid-drop model assuming that all the generated nucleus are in a liquid phase [5]. The homogeneous nucleation rate is represented by the equation (2) [6].

$$\beta_{ij} = \left(\frac{3v_1}{4\pi}\right)^{1/6} \sqrt{\frac{6kT}{\rho}\left(\frac{1}{i}+\frac{1}{j}\right)}\left(i^{1/3}+j^{1/3}\right)^2 \tag{2}$$

Where β_{ij} (m^3/s) is Brownian collisions between i-mers and j-mers, ρ(kg/m^3) is mass density. Because a collision between vapor molecules is assumed in this simulation, i and j are set to be 1. These equations can be applied when Knudsen number is more than 10. The homogeous nucleation rate J (m^3/s) is written as

$$J = N\frac{\beta_{11} n_1}{12}\sqrt{\frac{\Theta}{2\pi}}\exp\left[-\frac{4\Theta^3}{27(\ln S)^2}\right] \tag{3}$$

Where N (1/m^3) is a normalization constant written by

$$N = n_s \exp\Theta \tag{4}$$

Where n_s is the monomer concentration for the saturated vapor. And Θ is a dimensionless surface energy written as

$$\Theta = \frac{\sigma s_1}{k T} \tag{5}$$

Where s_1 is surface area of the monomer and k is the Boltzmann constant.

2.2 Heterogeneous Condensation Model of Primary Particle

When the particle growth is governed by the condensation of the vapor, an equation for the growth rate G expressed below can be obtained from a material balance over the growing particle [7].

$$G = \frac{da}{dt} = \frac{2}{\rho_c M} J_m \tag{6}$$

Where J_m is the mass flux of the condensable vapor, M is mass of molecular, and ρ_c is the molar density of the condensed phase. Because of the very small size of stable condensation nuclei, the Knudsen effect could play a meaningful role during their growth and should be accounted for in calculation of the mass flux. J_m is the equation (7) supporting the wide range of Knudsen number by Fuchs [8].

$$J_m = \frac{1+Kn}{1+1.7Kn+1.333Kn^2} \tag{7}$$

Where K_n is the Knudsen number defined as $Kn = \lambda/(a/2)$, λ is the mean free path of molecules of the condensing vapor. J_k calculated with equation (8) is the net flux of the vapor to the particle surface in the free molecular regime and comes from the kinetic theory.

$$J_k = \frac{1}{4}\rho_g\left(X - X^s\right)M\bar{v} \tag{8}$$

Where ρ_g is the molar density of the gas phase, $(X - X^s)$ represents difference of gas-phase mole fraction and equilibrium state mole fraction, $\bar{v}$ (m/sec) is mean molecular speed, and the superscript s means saturation conditions. Besides, J_k and J_m are identical only in the limit $K_n \to \infty$. Then, growth rate G is rewritten by equation (9) from equations (6) ~ (8).

$$G = \frac{4}{a}\frac{\rho_g}{\rho_c} D \left(X - X^s\right)\left\{\frac{1+Kn}{1+1.7Kn+1.333Kn^2}\right\} \tag{9}$$

Where ρ_g is the molar density of the condensation phase, D is diffusion coefficient, and λ is defined as $\lambda = 3D/\bar{v}$ from Meyer's equation [8].

2.3 Coagulation Model of Secondary Particle

(R1) The primary particles generated by the nucleation grow up through not only the condensation of iron atoms but also the coagulation caused by collisions between particles. In this model, the coagulation process is calculated by analyzing movements and collisions of particles distributed in the simulation region. A two-dimensional simulation region for the coagulation model is defined for time shorting. The size of the region is determined by the number density of primary particles obtained from the primary particle model to include 1000 particles in the region. The three dimensional number density of primary particles determined by the primary particle model is converted into the two dimensional number density by raising it to the 2/3th power. Secondary particles with various shapes and sizes are formed in the arc welding because the formation is very stochastic. However, only several or several tens of secondary particles are analyzed as examples of the formation in this simulation due to the limitation of the computational resource.

When the nucleation occurs, a primary particle is posted at a random position in the region and an initial velocity with a random direction is given to the particle. (R2) The initial velocity is determined from the thermal velocity calculated from the surrounding plasma temperature for simplicity. The sum of the momentums

is conserved through a particle collision. If particles collide at temperature above the melting point, they fuse into one spherical particle conserving their volumes. In other case, they attach each other like a chain shape depending on the temperature comparing with the melting point. A particle escaped from a boundary of the region is injected from the opposite boundary with the same velocity vector.

2.4 Calculation Condition

In this model, it is assumed the fume generated by helium GTA employing pure iron as a base metal. The cooling rate of 10^7K/sec which is determined by the plasma flow velocity and the plasma temperature gradient [9] and the iron vapor pressure of 10000Pa [10, 11] at the nucleation site are assumed. The calculation starts from 3000K and the temperature decreases until the room temperature of 300K with a cooling step of 0.5K. The main assumption is described as follows.

(1) The temperature of the condensation phase is equal to the plasma temperature.
(2) The heat generation by the condensation is ignored.
(3) The vapor is treated as an ideal gas.
(4) The primary particle is spherical.
(5) The collision of the particles happens between the maximum cross sections.

This model integrates the secondary particle model with the primary particle model. So, homogeneous nucleation, heterogeneous condensation, and coagulation could occur all together in each temperature.

In addition, it is calculated how surface tension affects particle size distribution as another point of view. It was calculated iron as a basic material and 0.5, 1, 2 N/m is used as surface tension. Surface tension is only changed. However this calculation is limited to primary particle calculation.

3. RESULT AND DISCUSSION

Fig. 1 shows dependence of iron partial vapor pressure and supersaturated vapor pressure on temperature. It was seen that, the nucleation occurs around 2100K mainly due to high degree of supersaturation and large amount of vapor is consumed by homogeneous nucleation and condensation.

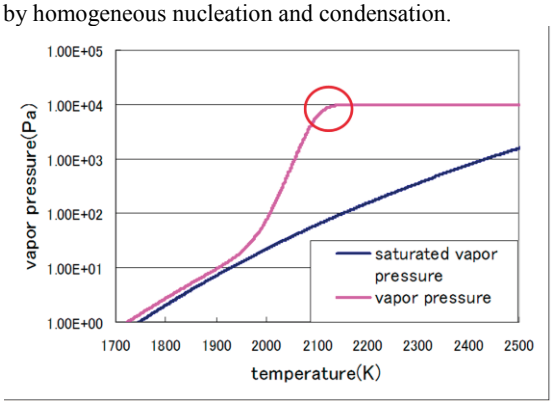

Fig. 1 Dependence of iron vapor pressure on temperature.

Fig. 2 expresses dependences of number densities of the primary particle and the secondary particle. The number of the primary particles increases around 2200K due to the nucleation. The secondary particle begins to form around 2150K a little behind the primary particle nucleation. Finally the primary particle is consumed by coagulation and disappeared almost of all around 1900K. Consequently only the second particles stayed below this temperature.

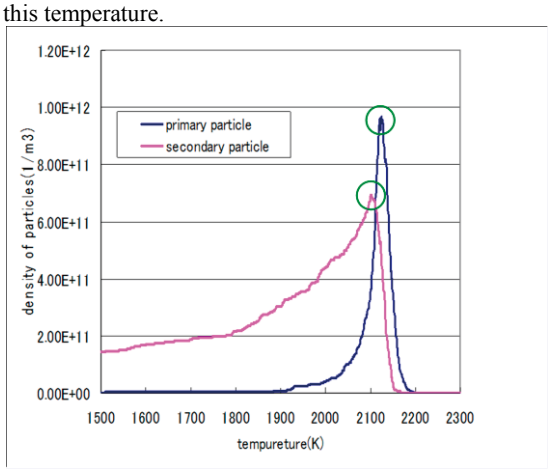

Fig. 2 Dependences of number densities of primary particle and secondary particle.

Fig. 3 ~ Fig. 5 show the particle distribution in the calculation domain in cases of 2100K, 1200K and 300K, respectively. The size of the domain is 6×10^{-7}m * 6×10^{-7}m. Fig. 3 shows the distribution at the temperature at which the nucleation begin to occur and Fig. 6 shows that at the room temperature at which the calculation is ended. In addition, Fig. 4 shows the distributions at the intermediate temperatures. It was seen that the homogeneous nucleation begin to occur and large amount of small primary particles whose sizes are mainly below 10nm are produced at 2100K. With decreasing temperature, the secondary particles are grown up by coagulation and condensation and the number of particles decreases. An average size of the secondary particles at 300K reaches 1.41×10^{-7} m.

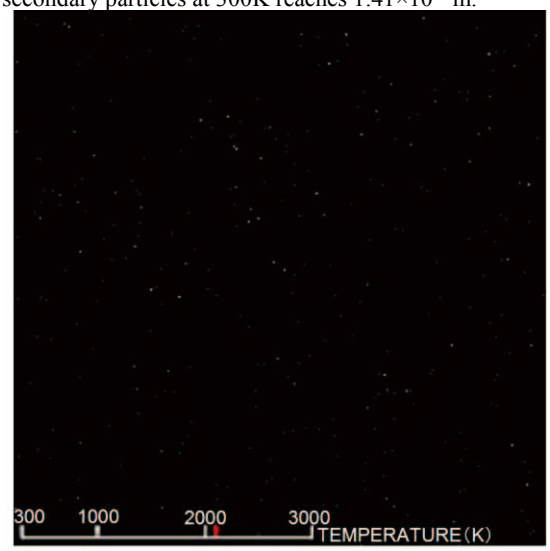

Fig. 3 Distributions of particles in cases of 2100K.

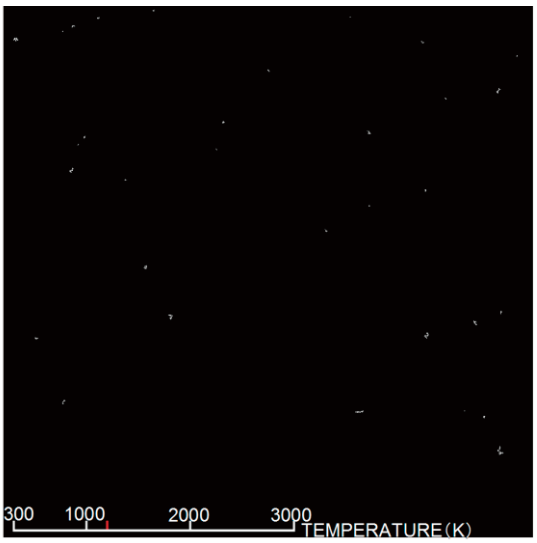

Fig. 4 Distributions of particles in cases of 1200K.

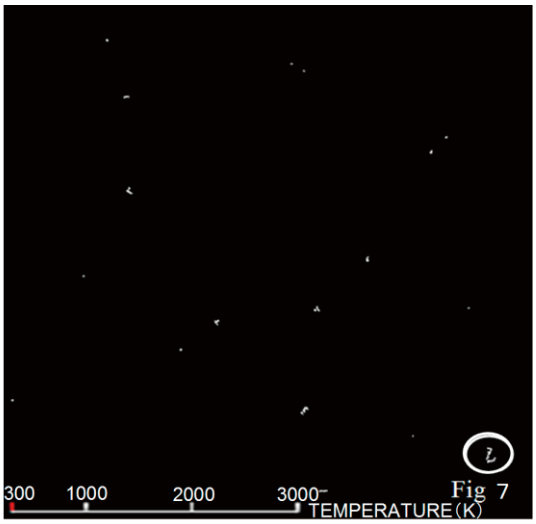

Fig. 5 Distributions of particles in cases of 300K.

Fig. 6 is a SEM image of the welding fume sampled in the experiment in the similar condition with the calculation. (R4) The experiment was conducted in a chamber filled with helium gas. The secondary particles with beaded (chain-like) shape composed of small particles whose sizes are approximately below 100nm were observed.

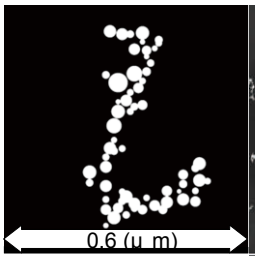

Fig. 6 Shapes of particles obtained from experimental result.

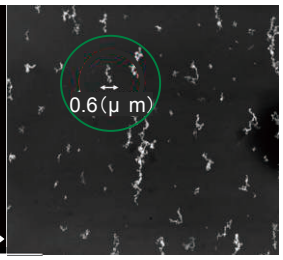

Fig. 7 Shapes of particles obtained from simulation result

Fig. 7 represents an enlarged picture of one of the secondary particles shown in Fig. 5 for observing a typical shape of those for an example. As a result, it was confirmed that the shapes and the sizes of the secondary particles obtained in the simulation approximately agrees with that in the experiment.

And Fig 8 shows the particle size distribution obtained from the calculation of surface tension effect. It was seen that with surface tension rising, particle diameter become larger. That is to say, the number of particle increases with increasing of surface tension and decreasing of vapor consuming by condensation per one particle.

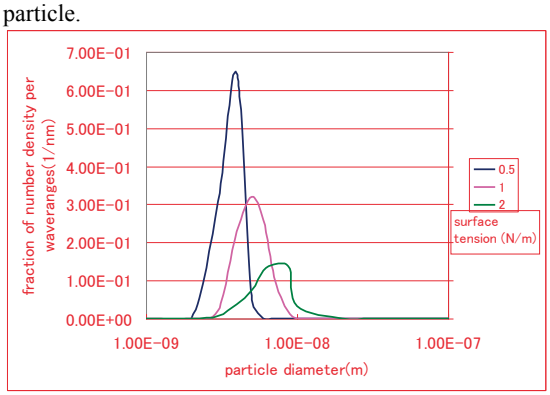

Fig. 8 Particle size distribution.

4. Conclusion

The integration model of a secondary particle model with a primary particle model was developed and the second particle coagulation process was visualized for observing the shapes of the secondary particle. As a result, it was confirmed that the shapes and the sizes of the secondary particles obtained in the simulation approximately agrees with that in the experiment.

References

[1] T. Watanabe, Y. Tamana, J. Plasma Fusion Res, 82 484-487 (2006).
[2] M. Shigeta, T. Watanabe, J. therm. spray technol, available online (DOI: 10.1007/s11666-009-9316-3).
[3] S. L. Girshick, C.P. Chiu, P. H.McMurry, Plasma Chemistry and Plasma Procesing,8 145-157 (1988), 2
[4] N. T. Jenkins, T.W. Eagar, Welding Journal, 84 87-s-93-s.(2005).
[5] S. K. Friendlander, Annals of the New York Academy of Sciences, 404 354-364 (1983).
[6] S. L. Girshick, C. P. Chiu, P. H. McMurry, Aerosol Sci. Tech,13:4 465-477 (1990).
[7] S. V. Joshi, Q. Liang, J Y. Park, J A. Batdorf, Plasma Chem. Plasma Process,10 339-358 (1990).
[8] N. A. Fuchs, A. G. Sutugin, International Reviews in Aerosol Physics and Chemistry, Vol. 2, G. M. Hidy and H. R. Brock, eds., PergamonPress, New York 361-368 (1971)
[9] S. Tashiro, M. Tanaka, K. Nakata T.Iwao, F. Koshiishi, K. Suzuki, K.Yamazaki, Science and Technology of Welding Joining, 12 (3) 202-207 (2007).
[10] H. Terasaki, M. Tanaka, M. Ushio, Metall.Mater.Trans A, 33A 1183-1188 (2002).
[11] H. Terasaki, M. Tanaka, M. Ushio, J. Weld. Soc., 20 201-206 (2002).
[12] The Japan institute metals ,edition No.3 date book of metals. 1993 Tokyo maruzen co.ltd(in japanese)

(Received January 7, 2009; Accepted February 15, 2010)